JOURNAL OF MATERIALS SCIENCE **34** (1999) 4285–4292

New investigations within the TeO_2-WO_3 system: phase equilibrium diagram and glass crystallization

S. BLANCHANDIN, P. MARCHET, P. THOMAS,
J. C. CHAMPARNAUD-MESJARD, B. FRIT
Laboratoire de Matériaux Céramiques et Traitements de Surface, ESA 6015, U.F.R. des Sciences, 123. Av. A. Thomas, 87065 Limoges Cedex, France
E-mail: frit@unilim.fr

A. CHAGRAOUI
Laboratoire de Chimie du Solide, Faculté des Sciences Ben M'Sik, B.P. 7955, Casablanca, Maroc

The TeO_2-WO_3 pseudo-binary system was investigated by temperature programmed X-ray diffraction and differential scanning calorimetry (DSC). The investigated samples were prepared by air quenching of totally or partially melted mixes of TeO_2 and WO_3. Glass forming compositions were identified by X-ray diffraction on quenched samples. Glass transition and crystallization temperatures were measured by DSC. The identification of the compounds appearing during glass crystallization revealed two new metastable compounds. The first one, which appears both for low WO_3 content and pure TeO_2 glasses, was attributed unambiguously to a new TeO_2 polymorph called γ. This one irreversibly transforms into the stable α-TeO_2 form, at about 510 °C. It crystallizes with the orthorhombic symmetry and unit cell parameters $a = 0.8453(3)$ nm, $b = 0.4994(2)$ nm, $c = 0.4302(2)$ nm, $Z = 4$. The second compound was detected for samples containing about 5 to 10 WO_3 mol %. It is cubic (F mode, $a = 0.569$ nm, $Z = 4$) and seems to have a fluorite-like structure. In addition, phase equilibrium diagram was determined. This binary system appears to be a true binary eutectic one.

1. Introduction

Tellurite systems including heavy element oxides, such as Tl_2O, Bi_2O_3 or WO_3, are interesting for optical glass formation. Glasses based on them are not hygroscopic and can be easily obtained transparent in the visible and near infrared regions (up to 5.5 μm). They exhibit low melting point ($\leq$800 °C), low glass transition temperature ($\leq$400 °C), high dielectric constant and interesting non-linear properties. They are therefore promising materials for optoelectronic devices and have been the subject, during the last few years, of numerous studies [1–10]. These investigations mainly concern their formation and some of their physical properties, but rarely take into account the chemical and equilibrium phase interaction of the components, which is nevertheless of primordial importance for the understanding of their thermal stability. In the case of the TeO_2-WO_3 glasses for example, their formation range [1–5], structure [11–15] and optical properties [2, 4, 6, 16–19] have been extensively investigated, whereas very little is available concerning their thermal stability and the corresponding phase equilibrium diagram. Published results report that the equilibrium diagram [20, 21] is of pure eutectic type (630 °C, 16.7 WO_3 mol %) and that the crystallization behaviour of glasses is complex, with several thermal events corresponding to the formation of unidentified compounds [15, 18, 22]. As part of a systematic study of optical glasses within the Bi_2O_3-TeO_2-WO_3 system, we therefore decided to re-examine the phase relation and the thermal stability of glasses within the TeO_2-WO_3 pseudo binary system. The present paper reports the results of this study.

2. Experimental

2.1. Samples preparation

All the crystallized samples were prepared by heating at 750 °C for 12 h and then 480 °C for 24 h, in gold crucibles, various intimate mixtures of reagent grade TeO_2 and WO_3 (purity higher than 99%).

For the glassy samples, the same mixtures were heated for half an hour at 850 °C in platinum crucibles. The melt was quickly cast onto a brass mould heated at about 60 °C, and quenched by pressing into thin sheets about 1.5 mm thick.

In order to increase the glass forming range towards TeO_2 and to check if pure TeO_2 glass can be obtained, as claimed by various authors [8, 11, 14, 15], samples containing 0 to 10 WO_3 mol % were quenched using the method proposed by Kim *et al.* [8]. The bottom of

the platinium crucible was quickly dipped in a freezing mixture, consisting of ice, ethanol and NaCl kept at $-10\,^{\circ}$C.

2.2. Samples characterization

Glass formation domain and identification of the crystallized phases were determined by X-ray diffraction (XRD) techniques using a Guinier De Wolff camera or a Siemens D5000 diffractometer (CuK_α radiation). The structural evolution with temperature of the glasses and crystallized compounds was followed by *in situ* XRD with a Siemens D5000 diffractometer (θ/θ, CuK_α radiation). This one was fitted out with a high temperature furnace (Anton Parr HTK 10), a platinum heating sample holder and an Elphyse sensitive position detector (14° aperture) allowing a quick data acquisition. The heating rate was $10\,^{\circ}\mathrm{C}\cdot\mathrm{min}^{-1}$, and each XRD pattern was recorded after an annealing time of 10 min at the choosen temperature.

Differential scanning calorimetry (DSC) experiments were carried out using a Netzsch STA 409 system (heat flux DSC). The experiments were performed in covered gold crucibles, using $5\,^{\circ}\mathrm{C}\cdot\mathrm{min}^{-1}$ heating and cooling rate, with carefully ground samples of about 30 mg. Crystallization (T_c) and melting (T_m) temperatures are onset temperatures determined at the intersection of the extrapolated baseline and the extrapolation of the linear part of the peaks. The glass transition temperatures (T_g) were taken as the inflection point of the step change of the calorimetric signal. The uncertainty of these temperatures is $\pm 5\,^{\circ}$C when DSC peaks are distinct but can be more important. The heats of crystallization δH were obtained from the area under the crystallization peak after heat flow rate calibration (calibration substance = sapphire).

The refractive indices of the glassy samples were determined with an optical microscope by successive focusing on the two parallel faces of polished samples. The densities were measured by helium pycnometry (Micromeritics Accupic 1330) on 30 mg powdered samples.

3. Results

3.1. Phase equilibrium diagram

The DSC and high-temperatue XRD results are consistent with the phase diagram shown in Fig. 1a. Because of the high TeO_2 losses for temperatures higher than 900 °C, the liquidus curve has not been determined for compositions containing more than 30 WO_3 mol %.

Only two invariant equilibrium were detected at $740 \pm 5\,^{\circ}$C and $622 \pm 5\,^{\circ}$C. They correspond respectively to the polymorphic transition: orthorhombic $WO_3 \Leftrightarrow$ tetragonal WO_3 [23] and to the eutectic reaction: liquid $\Leftrightarrow$ α-TeO_2 + orthorhombic WO_3. The eutectic composition (22 ± 1 WO_3 mol %) was determined by Tammann construction using the energies of the eutectic melting peaks (Fig. 1b). Contrary to the eutectic temperature, this value significantly differs from the previously proposed one (16.7 WO_3 mol %) [20, 21].

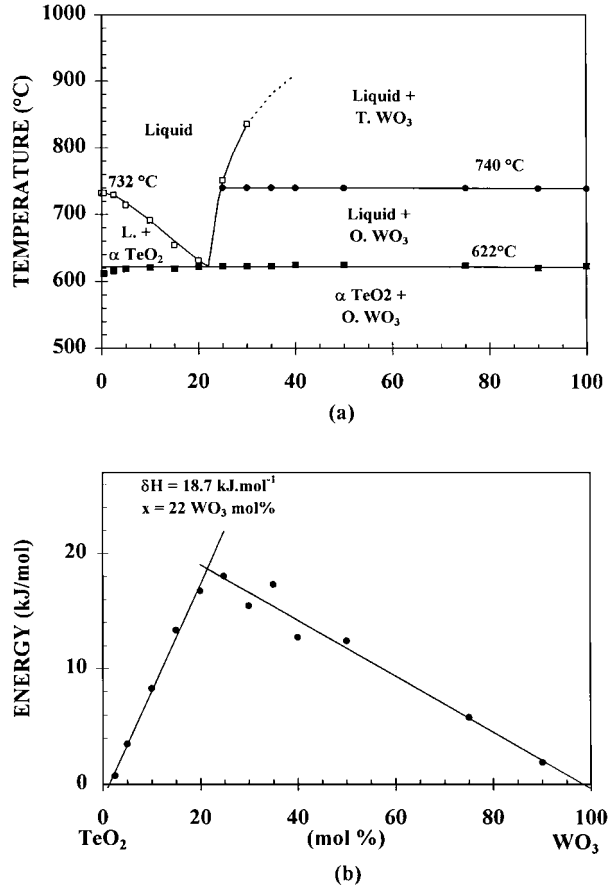

Figure 1 (a) Equilibrium phase diagram for the TeO_2-WO_3 system. (b) Tammann construction for this diagram.

The monoclinic $WO_3 \Leftrightarrow$ orthorhombic WO_3 transformation, which occurs at about 330 °C [23], was not detected by DSC, even for pure WO_3, probably because it corresponds to a second order phase transition [24].

On the Tammann diagram (Fig. 1b), the intersections of the melting energy lines with the composition axis (1.3 and 98.6 WO_3 mol %) are sufficiently near the pure component representation points, with respect to the estimated errors on composition (± 1 WO_3 mol %), to consider the existence of narrow solid solution domains very improbable. The phase diagram is probably of simple eutectic type and the only stable crystalline phases to be expected, after thermal annealing of glassy samples, are α-TeO_2 and monoclinic or orthorhombic WO_3.

3.2. Glass formation and physical properties

Under our quenching conditions, transparent and homogeneous glasses could be obtained for $[(100-x)\,TeO_2 + x\,WO_3]$ samples with compositions $10 \leq x \leq 30$. These results are consistent with those previously reported ($8 \leq x \leq 33$–44), the limits of the glass domain strongly depending on the glass preparation temperature and on quenching conditions [1–5]. By quenching the melts in a mix of ice, ethanol and NaCl, the glass forming domain could be extended up to pure TeO_2 as previously reported [8]. The color of this glasses changes from white to yellow and then light green with increasing WO_3 concentration.

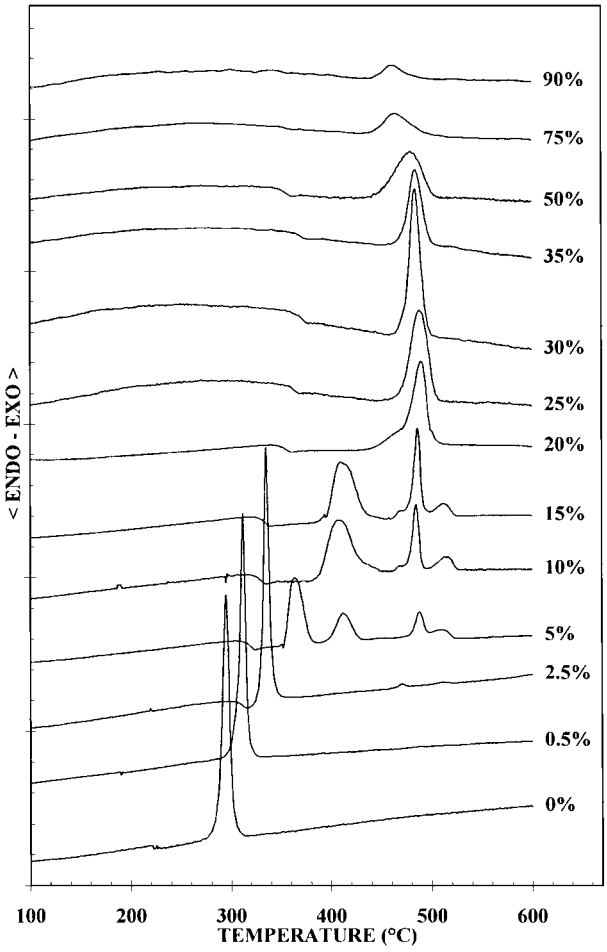

Figure 2 DSC curves of the glassy samples $(100-x)TeO_2 + xWO_3$.

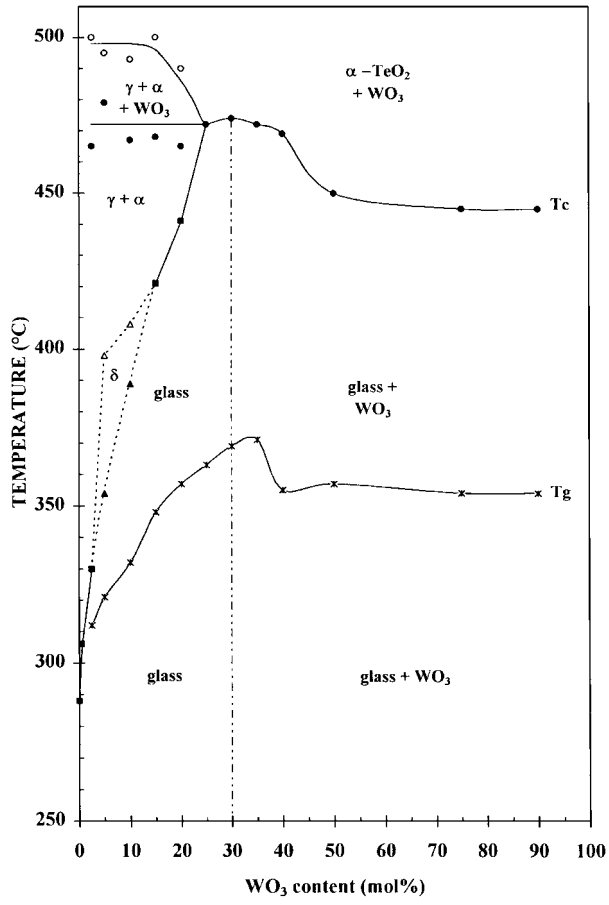

Figure 3 Evolution with composition of the glass transition temperature T_g (∗), of the various crystallization temperatures T_c (■: γ- and α-TeO_2; ▲: δ-phase, ●: WO_3) and of monotropic transition temperatures (△: $\delta \rightarrow \alpha$, ○: $\gamma \rightarrow \alpha$).

The refractive indices are in the range 2.2–2.3 and the density regularly increases from 5.84, for the pure TeO_2 glass, to 6.04 for $x = 0.25$. These values are in good agreement with previously reported ones [1–4].

3.3. Thermal behaviour of the glasses

Fig. 2 shows the DSC curves of various glassy samples with composition $0 \leq x \leq 90$. Those for which $0 \leq x \leq 30$ were pure glasses whereas those with $30 < x \leq 90$ were mixes of a glass with quasi constant composition ($x \approx 35$) and increasing quantities of crystalline WO_3.

In general, the curves show a step change of the baseline between 310 and 370 °C, which corresponds to the glass transition temperature T_g. For higher temperatures, one or several exothermic peaks are observed, whose significance was unambiguously determined by the temperature programmed XRD study. For the $x = 0$ and 0.5 samples, no glass transition was detected on DSC curves, probably because the corresponding thermal event was too close to the crystallization peak.

The thermal parameters (T_g, T_c and transition temperatures) estimated on DSC curves and the various crystalline phases detected at different temperatures by XRD are visualised in Fig. 3. Globally it is clear that the difference $T_g - T_c$, and so the thermal stability of glasses, regularly increases with the WO_3 content. The thermal behaviour strongly varies with composition. Four different domains can be distinguished.

(i) For very low WO_3 contents ($x \leq 2.5$), only one sharp and important exothermic peak is observed on the DSC curves. As shown in Figs 4 and 5, it corresponds to the simultaneous crystallization of α-TeO_2 and of an unknown compound. The formation of this unknown phase from pure TeO_2 glass strongly suggests that it should be a new metastable TeO_2 polymorph. So it will be called hereafter γ-TeO_2. It probably corresponds to the unknown crystalline phase noticed by Sekiya *et al.* in a previous study of the same glasses [15]. It disappears at about 480–500 °C to the benefit of the α-TeO_2 form. No thermal event was detected at the disparition of this phase for $x = 0$ and 0.5 samples, probably because of, on the one hand the low energy of this polymorphic transition, and on the other hand the small proportion of crystals concerned. However the third very small exotherm observed at 480–490 °C on the DSC curve of the $x = 2.5$ sample could perhaps account for it, the second one at about 460 °C corresponding, as we will see further, to the crystallization of small amounts of WO_3.

(ii) When $5 \leq x < 15$, four exothermic events are observed. The first peak ($T_c = 355$ °C for $x = 5$, $T_c = 388$ °C for $x = 10$) is associated with the crystallization of another new compound, with cubic symmetry, that we will call δ (Fig. 6). The second peak ($T \approx 400$ °C for $x = 5$) corresponds to the crystallization of γ-TeO_2, and to the decomposition of the δ phase into the stable α-TeO_2 polymorph. The third one (about 470 °C for

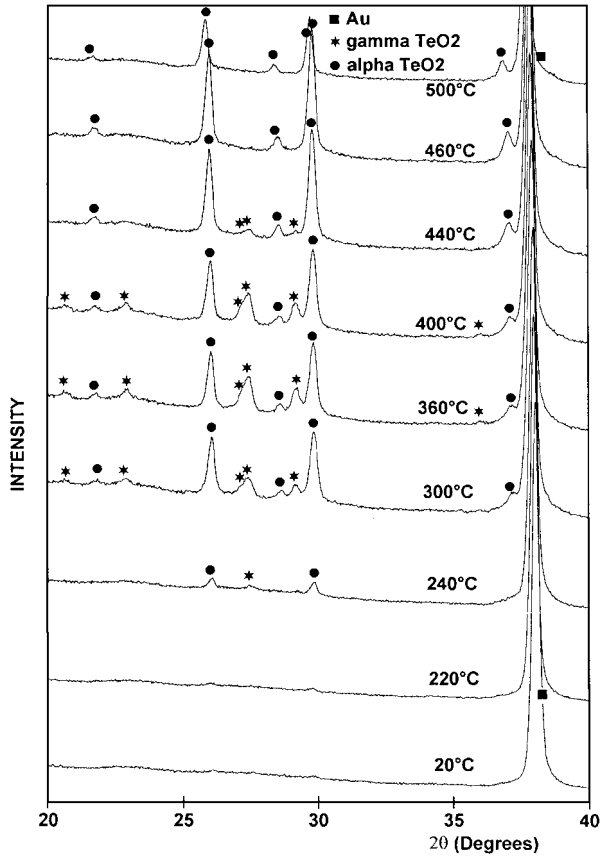

Figure 4 XRD powder pattern at various temperatures for a pure TeO_2 glass ($x = 0$).

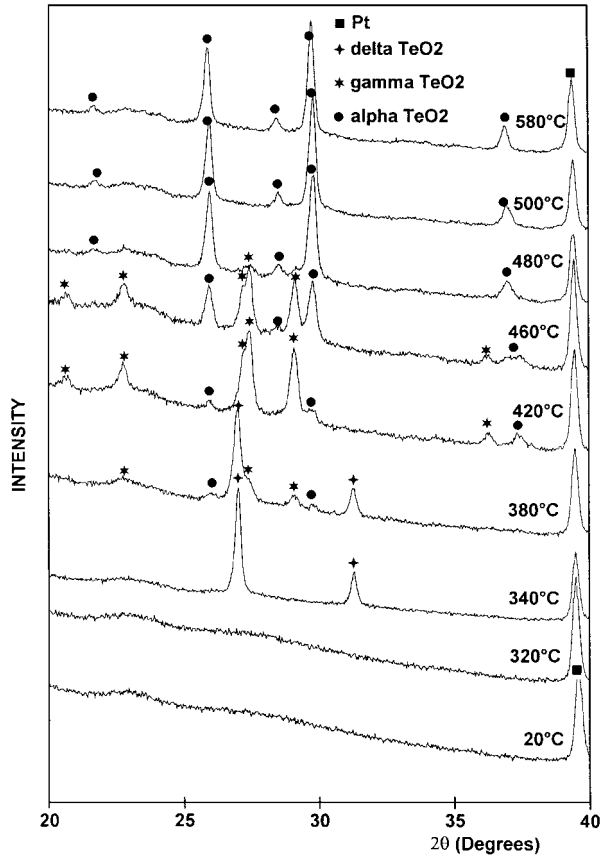

Figure 6 XRD powder pattern at various temperatures for a glassy sample containing $x = 5WO_3$ mol %.

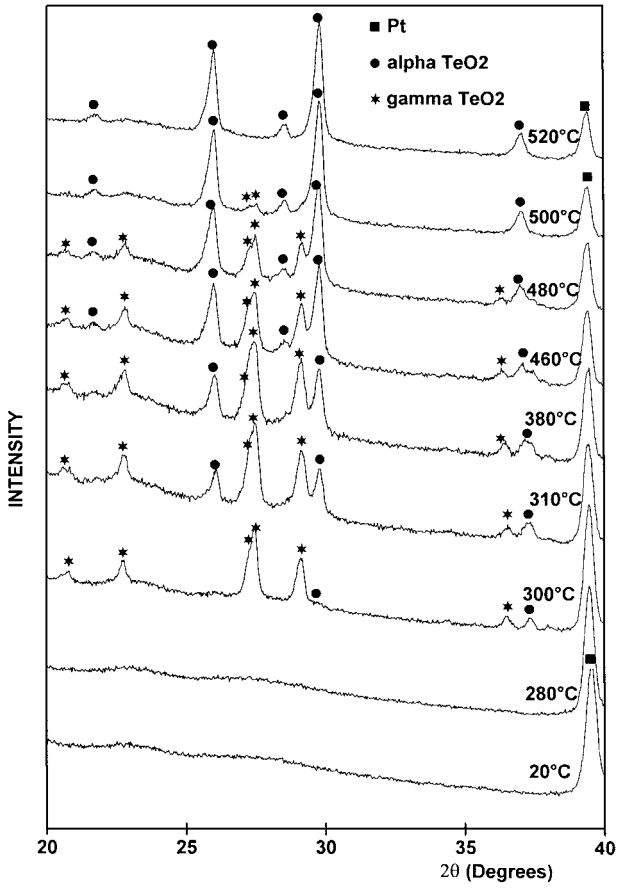

Figure 5 XRD powder pattern at various temperatures for a glassy sample containing $x = 2.5WO_3$ mol %.

all the samples) corresponds to the crystallization of WO_3. The last one, less intense, is associated with the transformation at about 490 °C of γ-TeO_2 into α-TeO_2.

(ii) For the samples with $x = 15$, the δ phase is no longer formed (see Fig. 7) and so only three peaks are observed on the DSC curves. They correspond successively to the crystallization of γ-TeO_2, the crystallization of WO_3 and the transformation $\gamma \rightarrow \alpha$. This composition seems to optimize the crystallization of the γ phase, the quantity of this phase progressively decreasing with increasing WO_3 content x.

(iv) When $x \geq 20$, only α-TeO_2 and WO_3 are formed. They crystallize at nearly the same temperature ($T \approx 460$ °C, see Fig. 8). So, only one distorted exothermic peak is observed on the DSC curves.

3.4. Identification and characterization of the new crystalline phases

TeO_2 is known to exist in two polymorphs at ordinary pressure and temperature: α-TeO_2 (paratellurite) and β-TeO_2 (tellurite) which is the natural metastable form [25–27]. Another polymorph, elaborated at high pressure (100 kbar, 800 °C), has been reported but without any information about its crystal structure [28]. None of these phases could be indentified with the new γ and δ phases by comparison of their respective XRD patterns. Considering the experimental conditions of the formation of these new crystalline phases, it was tempting to consider them as two new metastable polymorphs of TeO_2. In order to check this hypothesis, we have tried

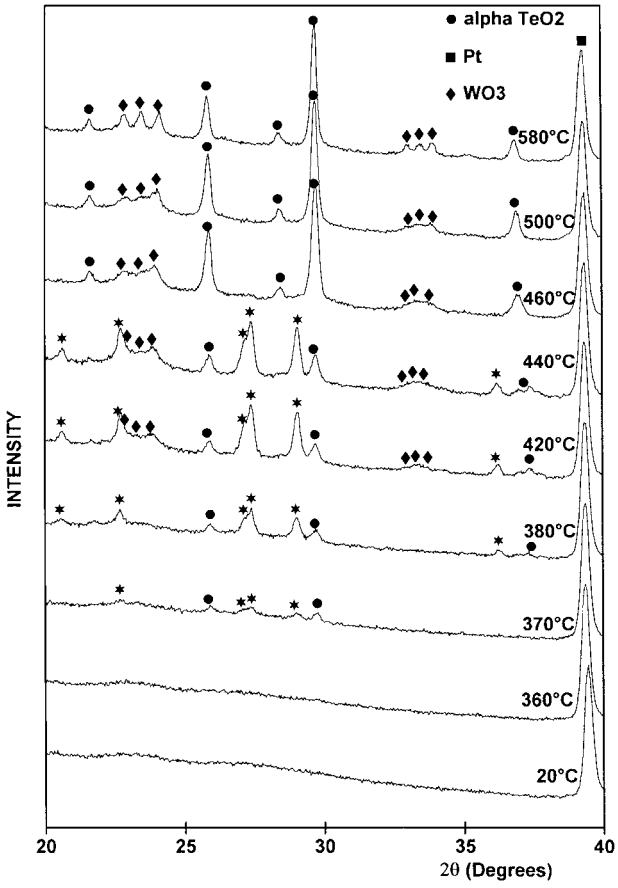

Figure 7 XRD powder pattern at various temperatures for a glassy sample containing $x = 15WO_3$ mol %.

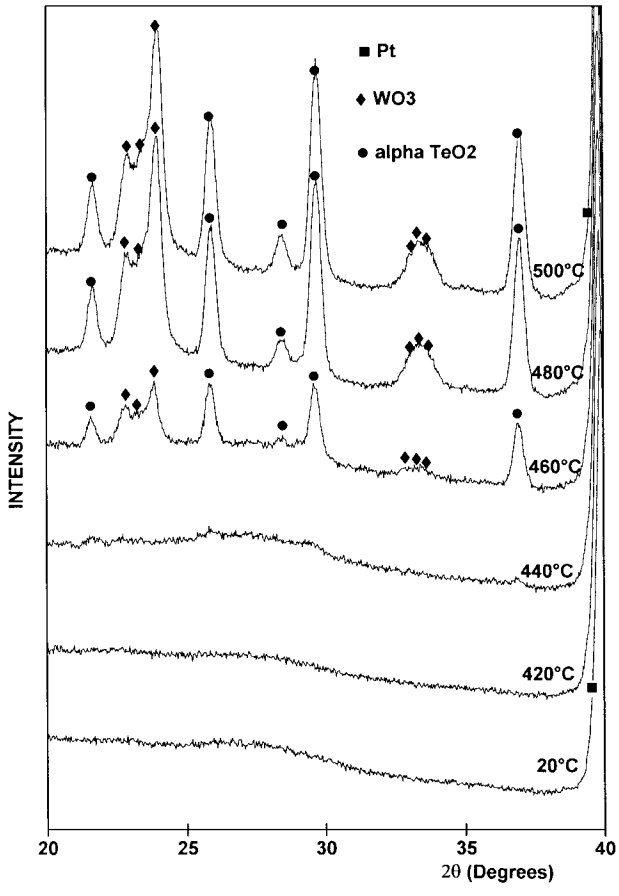

Figure 8 XRD powder pattern at various temperatures for a glassy sample containing $x = 25WO_3$ mol %.

to obtain them as pure as possible and to structurally characterize them.

3.4.1. The γ phase

Well crystallized γ-TeO_2 was obtained almost pure (only small amounts of the α form were detected on the XRD patterns) by slowly heating up to 390 °C a pure TeO_2 glass and then annealing for 24 h at this temperature. Its XRD pattern (Fig. 9) could be indexed (Table I) by using the automatic indexing programs ITO [29] and TREOR [30]. Both programs proposed an unique solution corresponding to an orthorhombic cell (possible space groups: P222, Pmm2 or Pmmm) with the following refined parameters (U-Fit program [31]): $a = 0.8453(3)$ nm, $b = 0.4994(2)$ nm,

TABLE I XRD powder data for γ-TeO_2

h, k, l	d_{obs} (Å)	d_{calc} (Å)	I/I_{max} (%)
110	4.298	4.300	12
200	4.222	4.226	6
101	3.829	3.834	11
11	3.255	3.259	70
210	3.224	3.226	100
111	3.037	3.041	24
201	3.012	3.015	34
211	2.579	2.581	2
20	2.496	2.497	15
120	2.396	2.395	3
301	2.356	2.357	2
002/220	2.149	2.150	3
400	2.111	2.113	1
102	2.084	2.084	6
410	1.945	1.946	2
221	1.922	1.923	15
401	1.897	1.897	1
212	1.788	1.790	4
411	1.772	1.773	14
321	1.714	1.714	4
130/022	1.629	1.630	3
312	1.618	1.617	13
420	1.613	1.613	6
510/122	1.600	1.599	6
31	1.552	1.553	3

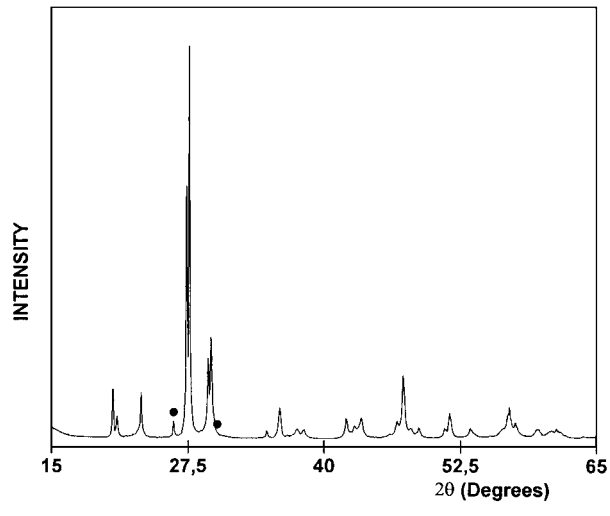

Figure 9 XRD powder pattern of the γ-TeO_2 polymorph obtained by annealing of a pure TeO_2 glass (● = α-TeO_2).

$c = 0.4302(2)$ nm and $V = 0.1816(2)$ nm^3 (values between parentheses are estimated standard deviations). The measured density ($d_{exp} = 5.80$) implies $Z = 4TeO_2$ units per cell ($d_{calc} = 5.84$). This density is lower than the value measured for the α form ($d = 5.97$) but very close to the value reported for the β form ($d = 5.75$–5.80) [32].

Since it was prepared from a pure TeO_2 glass, the new compound can, without any doubt, be considered as a new metastable polymorphic form of tellurium dioxide. Its obtaining, as the only crystalline phase, for a glass containing 15 WO_3 mol %, and the changes observed in the XRD pattern, allow to suppose that some tungsten oxide could be incorporated into the crystal structure. More accurate crystallographic studies are needed to check such an hypothesis.

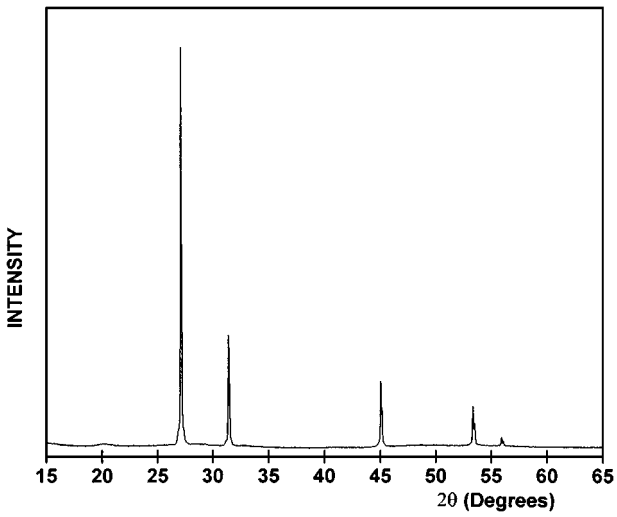

Figure 10 XRD powder pattern of the cubic δ phase obtained by annealing of a 95% TeO_2-5% WO_3 glass.

3.4.2. The cubic δ phase

Various attempts to prepare this phase from pure TeO_2 glassy samples were unsuccessful. It could however be prepared as the unique crystallized phase, mixed with some quantity of glass, by annealing for 24 h at 350 °C a glassy sample containing 5 WO_3 mol %. The XRD pattern (Fig. 10) could be unambiguously indexed (Table II) with a cubic cell (F mode, $a = 0.5690(1)$ nm). The measured density ($d_{exp} = 5.75$) implies $Z = 4TeO_2$ units per cell ($d_{calc} = 5.76$). This new compound has surely a fluorite-related structure of the same type as the cubic phase ($a = 0.554$ nm) formed by post-heat-treatment of glassy samples within the $15K_2O$-$15Nb_2O_5$-$70TeO_2$ system [33], as

TABLE II XRD powder data for δ-TeO_2

h, k, l	d_{obs} (Å)	d_{calc} (Å)	I/I_{max} (%)
111	3.282	3.285	100
200	2.843	2.845	28
220	2.010	2.012	20
311	1.715	1.716	11
222	1.642	1.643	2
400	1.422	1.422	<1
331	1.305	1.305	1
420	1.271	1.272	<1

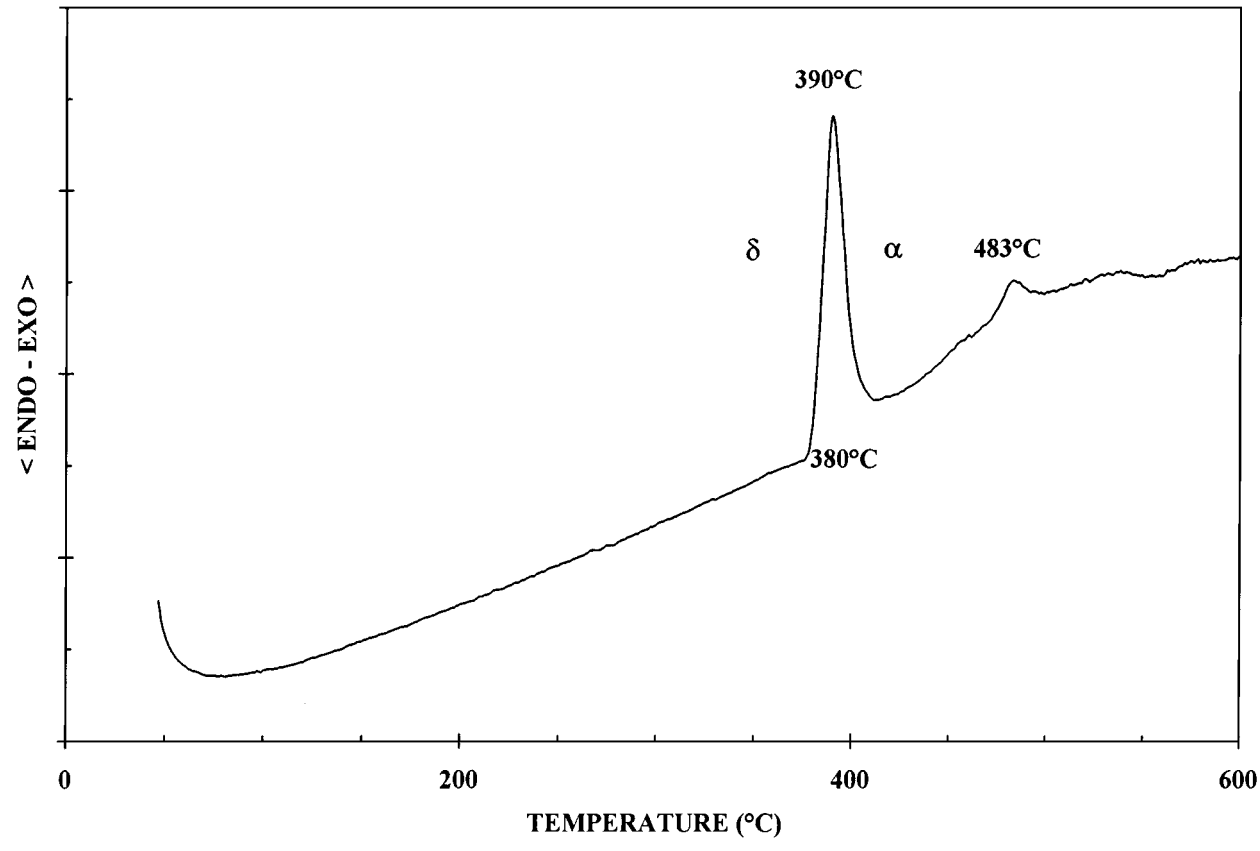

Figure 11 DSC curves of a 95% TeO_2-5% WO_3 glassy sample annealed 24 h at 350 °C. Contrary to the corresponding curve of Fig. 3, only two exothermic peaks are observed; they correspond to the $\delta \rightarrow \alpha$ transition (T ≈ 380 °C) and to the crystallization of small quantities of WO_3 (T ≈ 480 °C).

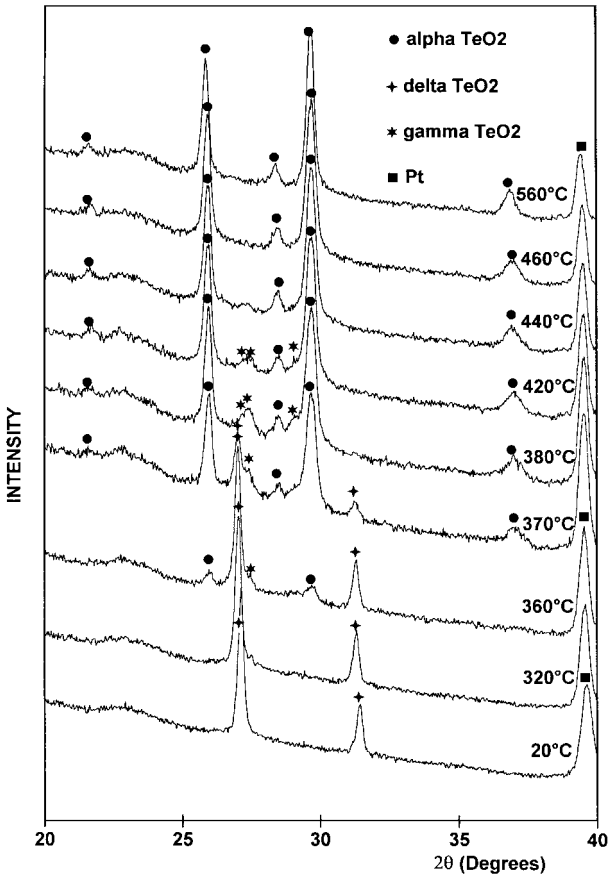

Figure 12 XRD powder pattern at various temperatures of a 95% TeO_2-5% WO_3 glassy sample annealed 24 h at 350 °C.

the anti-glass phases and other lanthanoid tellurates IV ($a = 0.570$–0.549 nm) reported by Trömel *et al.* [34], or as the metastable β polymorph of $Bi_2Te_4O_{11}$ ($a = 0.564$ nm) [35], part of a cubic nonstoichiometric phase $Bi_{1-x}Te_xO_{(3+x)/2}$ ($0.5 \leq x \leq 0.85$, $0.562 \leq a \leq 0.567$ nm) evidenced by El Farissi [36].

Although it was not possible to prepare this δ phase from pure TeO_2 samples, the identity of its unit cell parameters with the value ($a_F = 0.570$ nm) extrapolated from various solid solutions ($Pb_{1-x}Te_xF_{2-2x}O_{2x}$, $Bi_{1-x}Te_xO_{(3+x)/2}$ and $Cd_{1-x}Te_xF_{2-2x}O_{2x}$) to an hypothetical TeO_2 fluorite structure [37] allows to think that it could be a new fluorite-like metastable TeO_2 polymorph. Further experiments are in progress in order to confirm such an assertion.

However that may be, the DSC curve of Fig. 11 and the XRD patterns of Fig. 12 clearly confirmed that this metastable δ phase irreversibly transforms into the α form at about 380 °C.

4. Summary and conclusion

Study of various $[(100-x)TeO_2 + xWO_3]$ samples by differential scanning calorimetry and temperature programmed X-ray diffraction allowed us to determine the equilibrium phase diagram of the TeO_2-WO_3 pseudo-binary system. A binary eutectic was detected at 622 ± 5 °C and $x = 22$ WO_3 mol% ($\delta H = 19$ kJ·mol^{-1}). The thermal domain of investigation was limited to temperatures less than 900 °C because of high TeO_2 losses observed at higher temperatures.

The existence of a large glass-forming domain, whose extension strongly depends on quenching technique, has been confirmed. The thermal stability of those glasses decreases regularly with increasing TeO_2 content. So, TeO_2 rich glasses are very difficult to prepare and only very small quantities of pure TeO_2 glass could be obtained. Their thermal behaviour is complex and changes with composition.

In addition to stable α-TeO_2 and monoclinic WO_3 phases, two previously unknown compounds have been shown to crystallize from glasses with high TeO_2 content. The first one, called γ, has an orthorhombic unit cell. Since it was prepared from a pure TeO_2 glass, it can be considered as a new metastable form of TeO_2. The second one, called δ, has a cubic symmetry and is of fluorite-type. It is also metastable and seems to need some tungsten oxide to be stabilized.

More extra work are needed in order to master the precipitation of these two phases within the glassy matrix and to obtain transparent optical samples which could be efficient non-linear materials.

5. Acknowledgement

The authors gratefully acknowledge the "Conseil Régional du Limousin" for financial support.

References

1. J. E. STANWORTH, *J. Soc. Glass Technol.* **36** (1952) 217–241.
2. *Idem., ibid.* **38** (1954) 425–435.
3. A. K. YAKHKIND, *J. Amer. Ceram. Soc.* **49** (1966) 670–675.
4. W. VOGEL, H. BÜRGER, F. FOLGER, R. OEHRLING, G. WINTERSTEIN, H. G. RATZENBERGER and C. LUDWIG, *Silikattechnik* **25** (1974) 206–207.
5. V. KOZHUKHAROV, M. MARINOV and G. GRIGOROVA, *J. Non Cryst. Solids* **28** (1978) 429–430.
6. R. EL-MALLAWANY, *J. Appl. Phys.* **72** (1992) 1774–1777.
7. S. H. KIM, T. YOKO and S. SAKKA, *J. Amer. Ceram. Soc.* **76** (1993) 865–869.
8. *Idem., ibid.* **76** (1993) 2486–2490.
9. A. BERTHEREAU, Y. LE LUYER, R. OLAZCUAGA, G. LE FLEM, M. COUZI, L. CANIONI, P. SEGONDS, L. SARGER and A. DUCASSE, *Mater. Res. Bull.* **29** (1994) 933–941.
10. S. H. KIM and T. YOKO, *J. Amer. Ceram. Soc.* **78** (1995) 1061–1065.
11. V. DIMITROV, M. ARNAUDOV and Y. DIMITRIEV, *Monatshefte für Chemie* **115** (1984) 987–991.
12. V. KOZHUKHAROV, S. NEOV, I. GERASIMOVA and P. MIKULA, *J. Mater. Sci.* **21** (1986) 1707–1714.
13. Y. DIMITRIEV, V. DIMITROV, E. GATEV, E. KASHCHIEVA and H. PETKOV, *J. Non Cryst. Solids* **95/96** (1987) 937–944.
14. T. SEKIYA, N. MOCHIDA, A. OHTSUKA and M. TONOKAWA, *J. Ceram. Soc. Jpn.* **97** (1989) 1435–1440.
15. T. SEKIYA, N. MOCHIDA and S. OGAWA, *J. Non Cryst. Solids* **176** (1994) 105–115.
16. S. K. J. AL-ANI, C. A. HOGARTH and R. A. EL-MALAWANY, *J. Mater. Sci.* **20** (1985) 661–667.
17. H. TAKEBE, S. FUJINO and K. MORINAGA, *J. Amer. Ceram. Soc.* **77** (1994) 2455–2457.
18. I. SHALTOUT, Y. TANG, R. BRAUNSTEIN and A. M. ABU-ELAZM, *J. Phys. Chem. Solids* **56** (1995) 141–150.

19. I. SHALTOUT, Y. TANG, R. BRAUNSTEIN and E. E. SHAISHA, *ibid.* **57** (1996) 1223–1230.
20. A. K. YAKHKIND in "Structure and Physicochemical Properties of Inorganic Glasses," edited by A. G. Vlassov and V. A. Florinsk (Izd. Khimiya, Leningrad, 1974) p. 285.
21. V. V. SAFONOV, T. V. SMIRNOVA, D. V. BAYADIN, N. V. OVOHARENKO and N. R. SEMENOVA, *Russian J. Inorg. Chem.* **34** (1989) 1330–1334.
22. N. FORD and D. HOLLAND, *Glass Technology* **28** (1987) 106–113.
23. E. SALJE and K. VISWANATHAN, *Acta Cryst.* **A31** (1975) 356–359.
24. E. SALJE, *ibid.* **B33** (1977) 574–577.
25. H. BEYER, *Z. Fur Krist.* **124** (1967) 228–237.
26. O. LINSQVIST, *Acta Chem. Scan.* **22** (1968) 977–982.
27. P. A. THOMAS, *J. Phys. C: Solid State Phys.* **21** (1988) 4611–4627.
28. L. G. LIU, *J. Phys. Chem. Solids* **48** (1987) 719–722.
29. J. W. WISSER, *J. Appl. Cryst.* **24** (1969) 987.
30. P. E. WERNER, L. ERIKSSON and M. WESTDAHL, *ibid.* **18** (1985) 367–370.
31. M. EVAIN, unpublished programm, Institut des Matériaux de Nantes, UMR 110 CNRS, 2 Rue de la Houssiniere, 44072 Nantes Cedex 03, France.
32. H. LUMBROSO, "Compléments au nouveau traité de Chimie Minérale," Vol. 8: Tellure (Masson editor, Paris, 1977).
33. K. SHIOYA, T. KOMATSU, H. G. KIM, R. SATO and K. MATUSITA, *J. Non Cryst. Solids.* **189** (1995) 16–24.
34. M. TRÖMEL, W. HÜTZLER and E. MÜNCH, *J. Less-Common Met.* **110** (1985) 421–424.
35. Z. SZALLER, L. PÖPPL, G. LOVAS and I. DODONY, *J. Solid State Chem.* **121** (1996) 251.
36. M. EL FARISSI, PhD thesis, Université de Limoges, 1987.
37. A. IDER, J. P. LAVAL, J. CARRE, J. P. BASTIDE and B. FRIT, *J. Fluor. Chem.* **74** (1995) 141.

Received 31 October 1997
and accepted 2 March 1999